

Recycled poly(ethylene terephthalate) and its short glass fibres composites: effects of hygrothermal aging on the thermo-mechanical behaviour

Alessandro Pegoretti*, Amabile Penati

Department of Materials Engineering and Industrial Technologies, University of Trento, via Mesiano 77, 38050 Trento, Italy

Received 22 June 2004; received in revised form 23 August 2004; accepted 17 September 2004

Available online 1 October 2004

Abstract

This paper reports on the effects of hygrothermal aging at 70 °C in water and at 80% relative humidity, on the thermo-mechanical properties, molar mass and microstructure of recycled poly(ethylene terephthalate) (rPET) and its short glass fibres composites.

For all the investigated materials, the elastic mechanical properties (tensile and storage moduli) determined at low strain levels resulted practically unaffected by hygrothermal aging under the selected conditions. On the other hand, a marked reduction of the tensile strength and apparent fracture toughness has been observed for rPET matrix and its composites during hygrothermal aging, more markedly for materials immersed in water than for those aged at 80% RH. Both properties resulted to be related on the molar mass of the rPET matrix, that decreased during hygrothermal aging as a consequence of the hydrolysis process.

The materials glass transition, evaluated as the temperature of the loss factor peak, increased during hygrothermal aging due to the progressively restricted mobility of the amorphous phase caused by a concurrent crystallinity increase. This crystallization process (chemicrystallization) is favoured by temperature, by the plasticizing effect of water and by the reduction of molar mass.

Consistently with the mechanical measurements, the morphology of fracture surfaces exposed to hygrothermal aging in water revealed a reduction of plastic deformation of the rPET matrix and a weakening of the fibre–matrix interface for rPET composites.

© 2004 Elsevier Ltd. All rights reserved.

Keywords: Recycled PET; Hygrothermal aging; Thermal and mechanical properties

1. Introduction

Poly(ethylene terephthalate) (PET) is a thermoplastic polyester widely used in applications as diverse as textile fibres, films and moulded products [1]. While un-reinforced PET has a rather limited use as an engineering plastic, short fibre reinforced PET is increasingly used for high demanding applications, like windshield wiper arms, brake system, motor end frames, microswitches, coil forms, lamp sockets, oven handles, iron skirts, etc. [2]. One of the main reasons for the widespread use of PET is the possibility of producing a number of different grades over a broad range of molecular weights in a single multiproduct polymerization plant [3]. Moreover, among all plastics, PET has received

particular attention in terms of post-consumer recycling, due to the relatively large availability of PET bottles from special collection schemes [4]. In fact, the separation of PET bottles from municipal wastes represents one of the most successful examples of polymer recycling: in 2000, 187.4 kt of PET were recycled in Europe and most of them (70 kt) in Italy [5]. Numerous ways of recycling disposable beverage bottles have been reported [3], including methods for chemical recycling [3,6], such as methanolysis, glycolysis, hydrolysis, ammonolysis and aminolysis or physical recycling by re-melting [3,4,7–10]. After cleaning and grinding into flakes, the physical recycling of PET bottles involves re-melting of the solid flakes in an extruder for pelletization into chips or for direct melt processing into value added products (such as staple fibres, hollow fibres for fillings, partially oriented yarns, etc.) [3]. The performance of recycled PET can be improved by melt blending with

* Corresponding author. Tel.: +390461 882452; fax: +390461 881977.
E-mail address: alessandro.pegoretti@ing.unitn.it (A. Pegoretti).

reactive or non-reactive polymers [11], by adding additives, such as impact modifiers [11–14], flame retardants [15], mineral fillers [16] or by reinforcing with glass fibres [17]. Several studies have been published on the hygrothermal behaviour of virgin PET and its glass fibres composites [18–27] and of poly(buthylene terephthalate) and its glass fibres composites [28–35] but, to our knowledge, no information are available on the hygrothermal stability of recycled PET and its glass fibres composites under accelerated aging conditions.

Aim of this paper is to report on the effects of hygrothermal aging at 70 °C in water or at 80% relative humidity on the microstructure and thermo-mechanical properties of recycled PET and its short glass fibres composites.

2. Experimental

2.1. Materials and processing

Recycled poly(ethylene terephthalate) (rPET) pellets (density ISO 1183(A): 1.328 g/cm³; MVR ISO 1133 = 115 ml/10 min; intrinsic viscosity ISO 1628-5 = 0.70 dl/g) were produced by Eco Selekt Europa Srl (Salerno, Italy) starting from beverage bottles recovered from municipal wastes and crushed into flakes. Tests of contaminants performed on rPET flakes in accordance to UNI 10667 standard, indicated the presence of about 40 ppm of PVC and less than 20 ppm of poliolefins, respectively. Chopped strand E-glass fibres (SGF) type 952 produced by Saint Gobain–Vetrotex were used as reinforcing agent in percentage of 15 and 30% by weight (samples rPET-15GF and rPET-30GF, respectively). The initial length of the chopped fibres was 4.5 mm. All components, i.e. rPET, nucleating agent and short glass fibres were mixed in a single screw extruder (model EEGT/35/L-D36/ESI) working at 160 rpm and at temperatures in the range 280–310 °C. Before melt processing all components were carefully dried at temperatures in the range 100–130 °C for at least 4 h in order to limit the processing-induced hydrolysis.

Produced pellets were used for feeding a Sandretto

injection moulding machine, model 310/95, (barrel temperature range: 270–300 °C; injection pressure: 20 MPa; mould temperature: 130 °C) to produce:

- ASTM D638 dumb-bell specimens (length: 210 mm; thickness: 3.3 mm; gauge length: 80 mm; gauge width: 12.8 mm);
- rectangular test bars (length: 127 mm; width: 12.7 mm; thickness: 3.3 mm).

2.2. Conditioning of specimens

After moulding, all samples were conditioned for 3 months under laboratory conditions (23 °C, 40% RH.) until a constant weight was reached. The initial water content of samples reported in Table 1 was determined by evaluating their mass loss after drying at 120 °C under vacuum for 84 h. These annealing condition have been proven to be suitable to completely remove the excess of water from a 3.2 mm thick plate [36].

Specimens were then hygrothermally aged at 70 °C under two different conditions, i.e. (i) exposure of specimens to a humid environment (80% RH) and (ii) direct immersion of specimens in water (100% RH). The first condition was achieved by an ATS-FAAR mod. CU/220-35 humidostatic chamber set at 70 °C and 80% relative humidity. For the second condition, the specimens were totally immersed in a great surplus of distilled water (about 10 g of material per litre of water) at 70 °C in a Grant W38 thermostatic bath.

The aging process was followed up to 24 weeks for condition (i) and 32 weeks for condition (ii).

2.3. Sample characterization

Molar mass determinations were made by means of viscometric measurements performed at 25.0 °C with an Ubbelohde viscometer (type 1C) on diluted dichloroacetic acid/polymer solutions. All solutions were stirred for 45 min at 100 °C in order to obtain the complete dissolution of rPET specimens in the selected solvent. The relationship between intrinsic viscosity (IV in dl/g) and the number-average

Table 1
Some thermo-mechanical properties of un-aged rPET and its short glass fibre composites and of Rynite[®] 530 NC010

Property	Material			
	rPET	rPET-15GF	rPET-30GF	Rynite [®] 530 NC010
Temperature/value of the loss factor peak (°C)	92/0.177	92/0.057	94/0.053	93/0.052
HDT (°C)	80 ± 1	221 ± 2	232 ± 1	224 ^a
Tensile modulus (MPa)	3460 ± 230	7000 ± 140	11100 ± 490	11380 ± 580
Tensile strength (MPa)	34.1 ± 6.6	68.9 ± 1.7	120.0 ± 1.0	150.5 ± 1.7
Tensile strain at break (%)	1.17 ± 0.23	1.16 ± 0.04	1.40 ± 0.03	2.21 ± 0.12
Tensile energy to break (MJ/m ³)	0.25 ± 0.13	0.43 ± 0.03	0.95 ± 0.02	2.12 ± 0.17
K _{IQ} (MPa m ^{1/2})	1.49 ± 0.17	2.25 ± 0.10	4.58 ± 0.25	6.0 ± 0.1

^a Taken from Ref. [2].

molar mass (M_n in g/mol) under this condition is given by the following Mark–Houwink equation [37]:

$$IV = 6.7 \times 10^{-3} M_n^{0.47} \quad (1)$$

Specimens of rPET-15GF and rPET-30GF composites were dissolved in dichloroacetic acid at 100 °C and their fibre length distribution evaluated by an optical microscope and an image analyser system on about 100 fragments obtained after filtration of the solutions.

Tensile tests were conducted on the ASTM D638 injection moulded dumb-bell specimens, by an Instron model 4502 universal testing machine equipped with a 10 kN load cell, on at least five specimens. All tests were performed at a cross-head speed of 1 mm/min and the specimens elongation was monitored by an Instron model 2620 clip-on extensometer with a gage length of 25 mm.

Fracture toughness measurements were conducted on single-edge-notch bending (SENB) specimens in accordance to ASTM D5045 standard [38], by an Instron model 4502 universal testing machine, on at least three specimens. SENB specimens (thickness $B=3.3$ mm, width $W=9$ mm and length $L=40$ mm) were machined out from the injection moulded rectangular test bars and razor notched to an a/W (crack length to width ratio) of about 0.5 and tested under a three point bending configuration with a span to width ratio of 4, at a cross-head speed of 10 mm/min. For bend specimens with $S/W=4$ the fracture toughness (K_{IC}) is as follows:

$$K_{IC} = \frac{P_{\max}}{BW^{1/2}} f\left(\frac{a}{W}\right) \quad (2)$$

where P_{\max} is the maximum load, and $f\left(\frac{a}{W}\right)$ is a calibration factor depending on the specimen geometry [38].

The fracture surfaces of SENB specimens, which were approximately perpendicular to the direction of injection, were sputtered with gold and observed with a scanning electron microscope (Cambridge, model Stereoscan 200). Observations were made at an accelerating voltage of 20 kV.

Dynamic mechanical thermal analysis (DMTA) tests were conducted in a tensile loading mode, by a Polymer Laboratories dynamic mechanical thermal analyzer (model MkII) on strips (thickness 3.3 mm, width 1.8 mm and length 25 mm) machined out from the injection moulded rectangular test bars. All measurements were performed with a peak to peak displacement of 32 μm , in a temperature range from 0 up to 200 °C, at a heating rate of 3 °C/min and at a frequency of 1 Hz.

Heat distortion temperature (HDT) was measured by an ATS-FAAR MP3 instrument on three specimens simultaneously. In accordance to ASTM D 648-1 standard, specimens have been tested in the edgewise position under a flexural load giving a maximum fibre stress of 1.82 MPa at a heating rate of 120 °C/min.

3. Results and discussion

3.1. Microstructure and properties of un-aged sample

SEM micrographs of fracture surfaces of rPET, rPET-15GF and rPET-30GF samples are reported in Figs. 1 and 2. At a macroscopic level rPET appears as a relatively compact material (Fig. 1(a)), while an inspection at higher magnification levels (Fig. 2(a)) evidences the

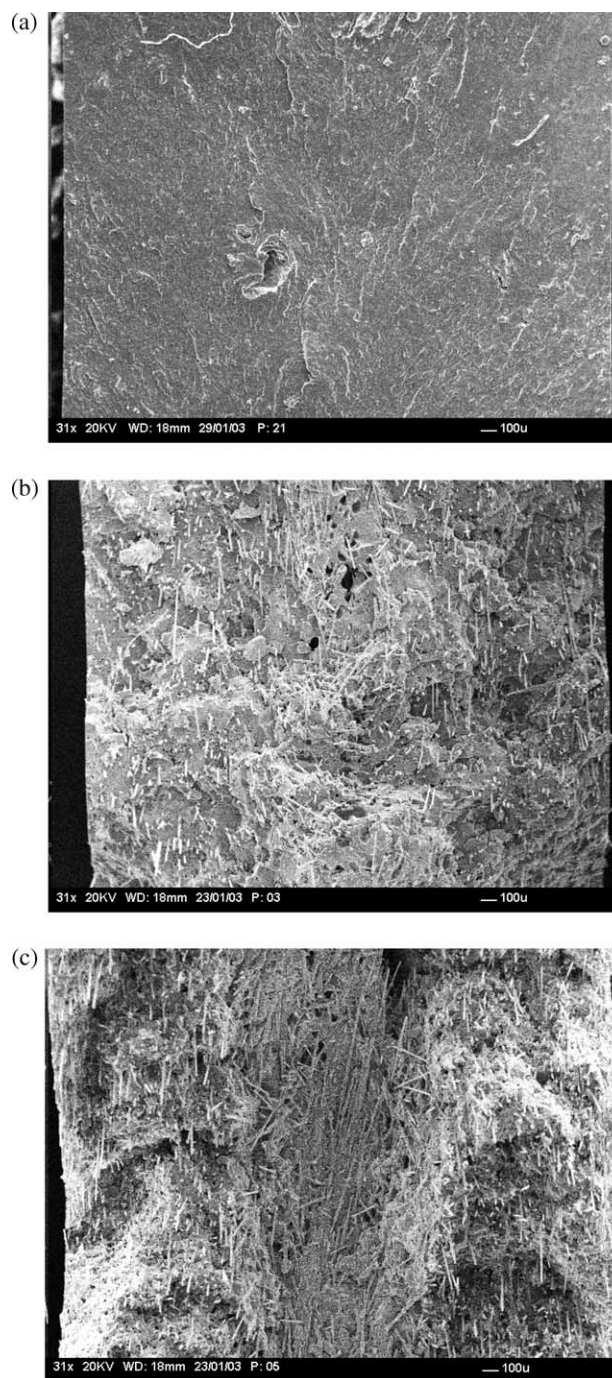


Fig. 1. Scanning electron micrographs of fracture surfaces of un-aged materials: (a) rPET, (b) rPET-15GF and (c) rPET-30GF.

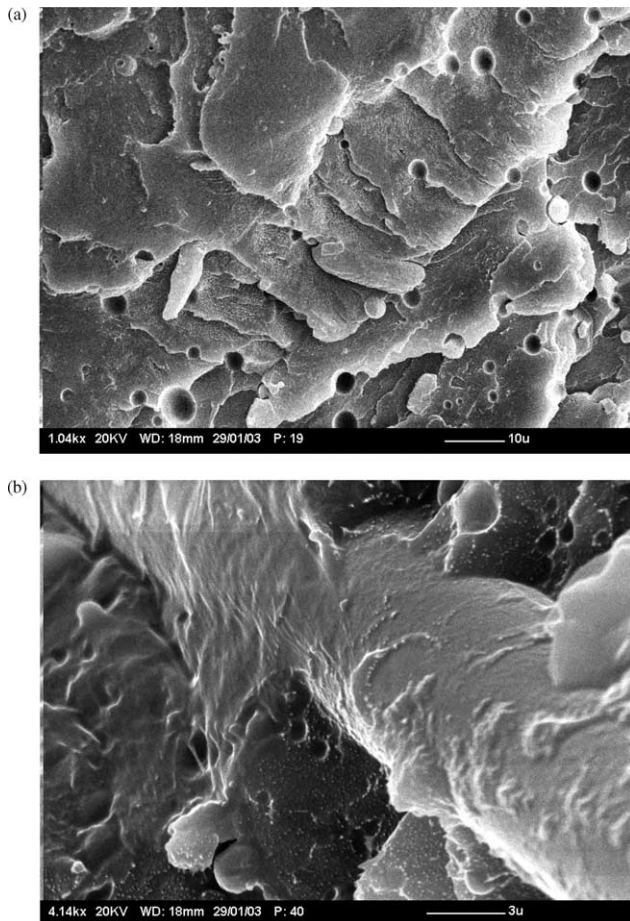


Fig. 2. Scanning electron micrographs of fracture surfaces of un-aged materials: (a) rPET and (b) rPET-30GF.

presence of holes of dimensions in the range 1–6 μ . The origin of these defects could be related to the moulding conditions and in particular to the elevated mould temperature (130 °C) required to obtain fully crystallized specimens. The micrographs of rPET-15GF and rPET-30GF composites (Fig. 1(b) and (c)) indicate the presence of a skin-core morphology, that is particularly evident for the sample with the highest fibre content. The processing-induced skin-core structure in injection moulded short fibre reinforced thermoplastics has been widely documented [39,40]. This generally consists of a three-layer laminate structure across the specimen thickness, with layers containing fibres, which exhibit different orientations. In the outer layers the fibres are roughly oriented along the mould filling direction (MFD), while in the central layer fibres are more or less perpendicular to this direction. In the present case, it is evident that the skin-core orientation difference is very weak for the rPET-15GF but becomes very important for specimens reinforced with 30 wt% of short glass fibre. As reported in Fig. 2(b), the level of fibre–matrix adhesion seems to be satisfactory as documented by the good spreading of the rPET matrix

onto the glass fibres surface and the absence of fibre–matrix debonding.

Table 1 shows the values of some selected thermo-mechanical properties of rPET and its short glass fibre composites obtained in this study and of a commercially available virgin PET reinforced with 30 wt% of short glass fibres (Rynite[®] 530 NC010 by DuPont). The properties of Rynite[®] 530 NC010 have been evaluated on ISO-527 dumb-bell specimens kindly supplied by DuPont de Nemours Italiana (Milano, Italia), following the procedures described in Section 2.3. The main differences between recycled and virgin materials are represented by the lower values of the ultimate tensile properties (strength and strain at break) that could be related to several factors, such as the presence of the small voids in the rPET matrix (see Fig. 2(a)) or possible differences in the molecular weight, fibre/matrix adhesion and fibre length. Fig. 3 reports the fibre length distribution evaluated on fibres extracted from reinforced rPET specimens. Due to the shear stresses related to the processing steps (extrusion and injection moulding), the fibre degraded from their initial length of 4.5 mm to average fibre lengths of 0.71 ± 0.14 mm and 0.55 ± 0.08 mm for rPET-15GF and rPET-30GF, respectively. Even if a marked fibre length reduction is occurring, the measured values are significantly higher than those reported by Yow et al. [35] for rubber-toughened short glass fibre reinforced PBT specimens melt processed via twin-screw extrusion and injection moulding. It is worth noting that the fibre length reduction is more severe as the fibre content increases, due to the increased fibre–fibre interactions.

3.2. Effects of aging on the mechanical behaviour: tensile tests and fracture toughness

The appearance of the tensile stress–strain curves of rPET-30GF sample un-aged and hygrothermally aged at

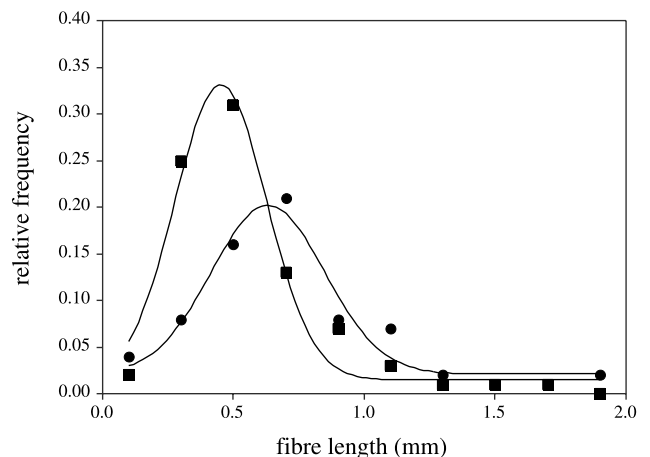


Fig. 3. Fibre length distribution of (●) rPET-15GF and (■) rPET-30GF. Solid lines represent data fitting with Gaussian function.

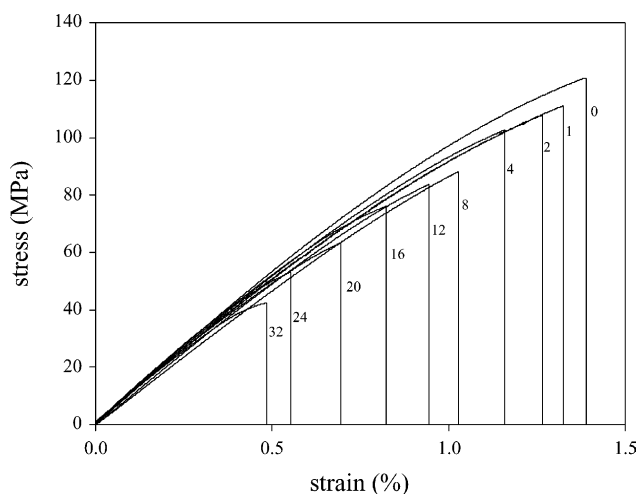


Fig. 4. Tensile stress–strain curves of rPET-30GF composites. Numbers refer to the weeks of immersion in water.

70 °C in water is shown in Fig. 4. It is clearly evident that the main effect of hygrothermal aging is a progressive reduction of the strength and strain at break values while the initial slope of the curves remains substantially unaffected. This general trend has been already observed for various materials, such as short glass fibre reinforced PBT hygrothermally aged in water up to 80 °C [33,34], Bis-GMA/TEGDMA resin reinforced with long glass fibres and hygrothermally aged in water up to 70 °C [41], poly(L-lactic acid) fibres hygrothermally aged in water at 37 °C [42]. The shape of the stress–strain curves of rPET and rPET-15GF samples is very similar to those of rPET-30GF sample and hence not reported. A summary of the effects of hygrothermal aging at 70 °C in water and at 80% relative humidity, on the tensile modulus and tensile strength of rPET and its short glass fibre composites is reported on Fig. 5(a) and (b), respectively. While the tensile modulus is practically constant over the entire degradation period, the strength is markedly decreasing. In particular, the strength reduction of sample immersed in water is more enhanced than for the sample exposed to 80% RH. Due to the hydrolysis of the ester linkage, molar mass of rPET is decreasing during hygrothermal aging: the variation of number-average molar mass during aging at 70 °C and 80 or 100% RH has been reported in a previous paper [43] and will not be discussed here. The observed molar mass decrease has been successfully modelled as a pseudo first-order reaction whose kinetics constant depends on the humidity conditions (i.e., on the concentration of water in the material). It is well known that molar mass affects the strength of polymers [44,45], the most important effect being the reduction of brittle strength with decreasing molar mass. Flory [44] has found that the tensile strength (σ_b) of cellulose acetate fractions depends on the number-average molar mass (M_n) according to the relation:

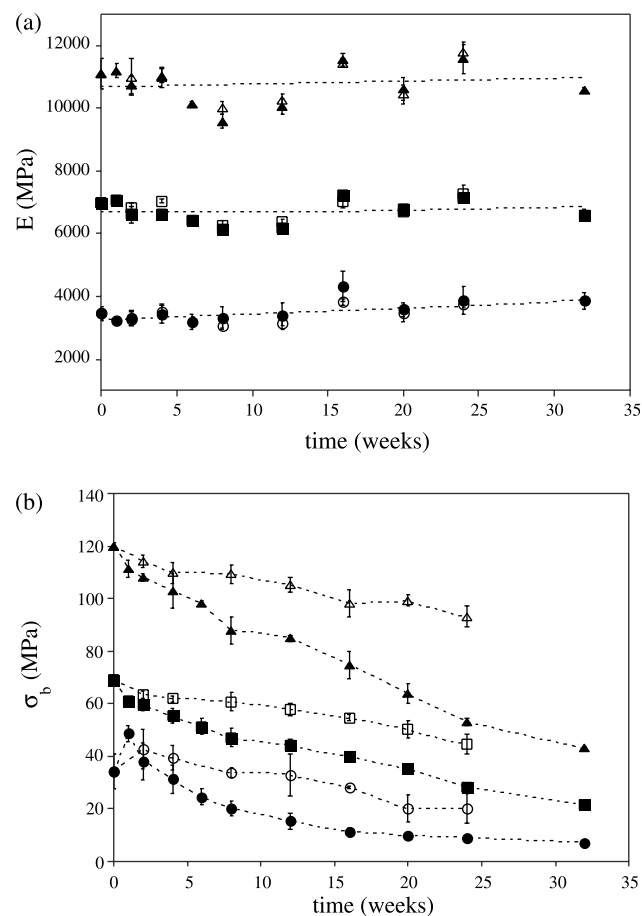


Fig. 5. Effects of hygrothermal aging on (a) tensile modulus E and (b) tensile strength σ_b for: rPET at (○) 80% RH or (●) immersed in water; rPET-15GF at (□) 80% RH or (■) immersed in water; rPET-30GF at (△) 80% RH or (▲) immersed in water.

$$\sigma_b = \sigma_b^\infty - \frac{A}{M_n} \quad (3)$$

where σ_b^∞ is the limiting tensile strength for very high molar mass and A is a constant evaluated with the aid of experimental data. Although Eq. (3) was proposed to encompass the effect of molar mass on the tensile strength of materials undergoing brittle fracture [44,45], it seems to be quite general [46]. In Fig. 6 the tensile strength values of rPET and its short glass fibre composites are plotted against the reciprocal of the number-average molar mass of rPET matrix experimentally evaluated during aging. It is worthwhile to note that data obtained under different humidity conditions tend to follow a common trend, thus indicating that tensile strength depends on the molar mass and not on the way this is reached. Moreover, data points agree reasonably well with the trend predicted by Eq. (3) even if a slope change is evident for molar masses in the range 6000–7000 g/mol. This effect could be tentatively explained by considering that, two phenomena are concurrently occurring during hygrothermal aging of the investigated materials. In fact, as evidenced by DSC measurements [43],

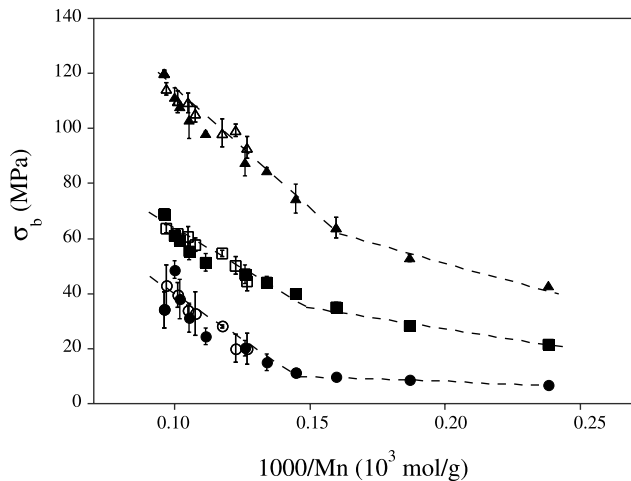


Fig. 6. Tensile strength values as a function of the reciprocal of the number-average molar mass of rPET matrix for: rPET at (○) 80% RH or (●) immersed in water; rPET-15GF at (□) 80% RH or (■) immersed in water; rPET-30GF at (△) 80% RH or (▲) immersed in water.

the molar mass decrease due to hydrolysis is accompanied by a crystallinity increase due to a chemicrystallization process. This process has been previously reported on virgin PET [20,22,23] and widely observed even on biodegradable semicrystalline aliphatic polyesters [42,47–52]. It can be explained by considering that chain scission in the amorphous phase may release previously entangled chain segment that become sufficiently free to find a spatial rearrangement into the crystalline phase. Molar mass decrease and crystallinity increase are likely to have opposite effects on the tensile strength that could account for the observed trend.

Fracture toughness tests performed on SENB specimens do not allow the determination of a critical value of the stress intensity factor in the framework of a linear elastic fracture mechanics approach. In fact, in most cases, the non-linearity was not within the specific (5%) reduction in the slope of the load-displacement curves recommended by the ASTM D5045 standard [38]. Apparent fracture toughness K_{I0} values have been still determined according to the above ASTM standard [38] and reported as a function of hydrothermal aging time in Fig. 7(a). It is interesting to observe that, under both the humidity conditions (80 or 100% RH) adopted for the hydrothermal aging at 70 °C, a marked decrease of the fracture toughness of the investigated materials is occurring. It has not been possible to perform fracture toughness measurements on un-reinforced rPET matrix immersed in water for more than 12 weeks since specimens became too brittle to be notched. There have been several studies of the dependence of the critical strain energy release rate, G_{IC} , upon molar mass for glassy polymers such as poly(methyl methacrylate), polystyrene and polycarbonate (for a review see [53,54]). In glassy polymers the general dependence of G_{IC} upon molar mass M is sigmoidal [53,54]. When M is low the polymer has a very low fracture energy, as the molar mass increases there is a

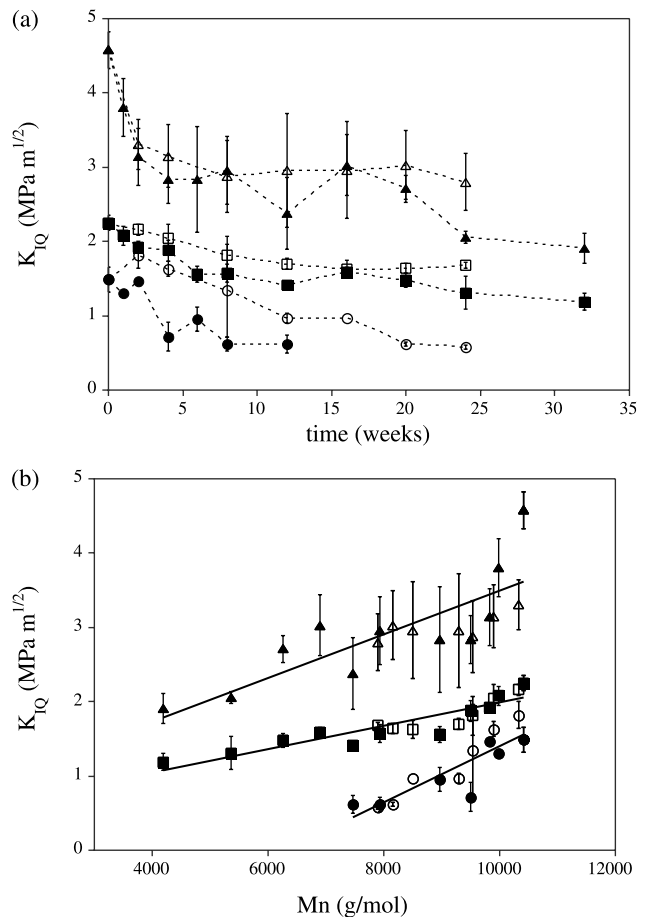


Fig. 7. Apparent fracture toughness values, K_{I0} , as a function of (a) hydrothermal aging time and (b) number-average molar mass of rPET matrix for: rPET at (○) 80% RH or (●) immersed in water; rPET-15GF at (□) 80% RH or (■) immersed in water; rPET-30GF at (△) 80% RH or (▲) immersed in water.

sudden rapid rise in G_{IC} until it levels off at a limiting value for very high molar mass. In other words, G_{IC} values are proportional to M^p where the exponent p can vary from 0.5 up to 3 or more, depending on the molar mass region [53]. A predictive model proposed deGennes [55] suggests that the fracture energy G_{IC} of glassy polymers is scaling roughly like M^2 , provided that the molar mass M be smaller than a certain limit M^* above which chain scission dominates and G_{IC} becomes independent of M . Since, K_{IC} is related to G_{IC} via [56]:

$$K_{IC}^2 = G_{IC} E' \quad (4)$$

with $E' = E$ for plane stress and $E' = \frac{E}{1-\nu^2}$ for plane strain conditions, where ν is the material Poisson's ratio, the model proposed by deGennes [55] predicts a linear dependence of K_{IC} on the molar mass. On the other hand, information about the influence of molar mass on fracture toughness of semicrystalline polymers are quite scarce in the scientific literature [56–58]. On Fig. 7(b) the apparent fracture toughness values are reported as a function of the rPET matrix number-average molar mass as determined

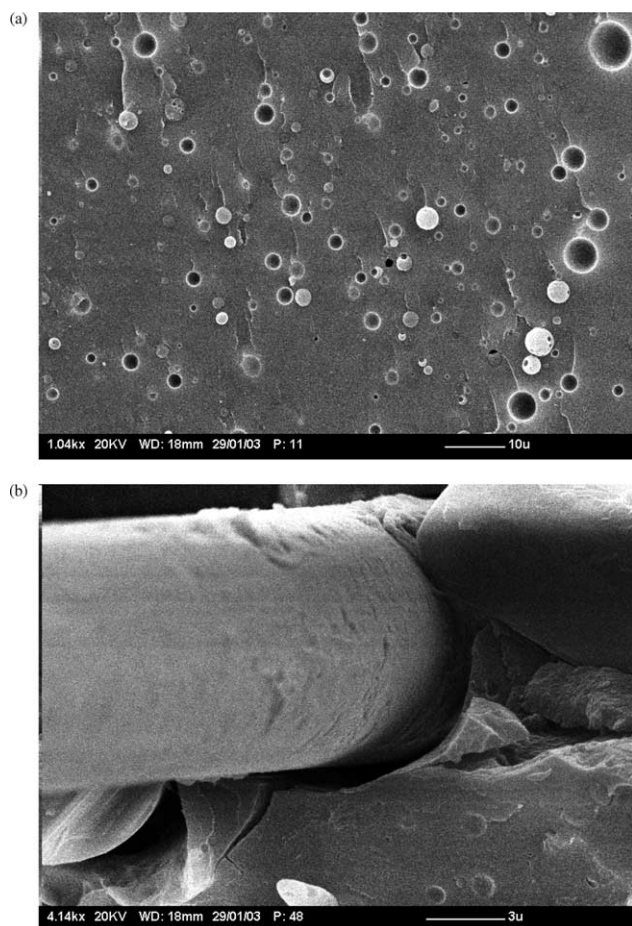


Fig. 8. Scanning electron micrographs of fracture surfaces of (a) rPET and (b) rPET-30GF specimens hydrothermally aged in water for 24 weeks.

by intrinsic viscosity measurements. Solid lines represent linear regression of experimental data. It is interesting to observe that, as for tensile strength, K_{IQ} values tend to follow a common line thus indicating that fracture toughness depend on the molar mass and not on the way this is reached. Moreover, a linear dependence on M_n is quite satisfactory followed by the experimental data, in accordance with the model proposed by deGennes [55].

The embrittlement of the rPET matrix due to hydrothermal aging is also evident from the change in the morphology of the fracture surfaces. In fact, as documented in Fig. 8(a), the fracture surface of unreinforced rPET after immersion in water at 70 °C for 24 weeks clearly results much smoother (i.e. with a lower degree of plastic deformation) than the corresponding unaged material (see micrograph of Fig. 2(a)). A SEM micrograph of rPET-30GF composite after hydrothermal aging in water for 24 weeks is reported in Fig. 8(b). In comparison to the unaged material (see Fig. 2(b)) the observation of the fracture surfaces put in evidence some matrix cracking and a marked weakening of the fibre–matrix interface resulting in a fibre–matrix debonding.

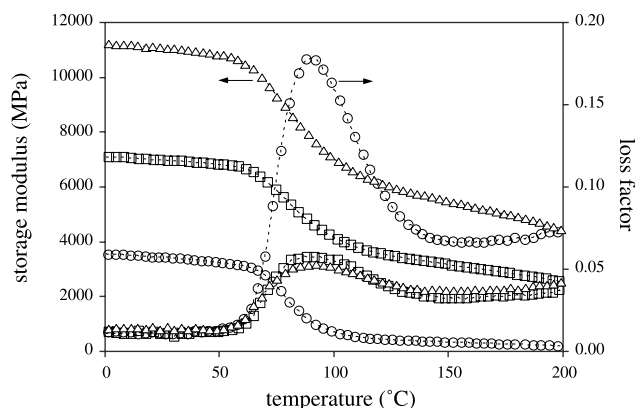


Fig. 9. Storage modulus and loss factor of un-aged (○) rPET, (□) rPET-15GF and (△) rPET-30GF specimens.

3.3. Effects of aging on the thermal behaviour: DMTA and HDT

The temperature dependence of storage modulus and loss factor of un-aged rPET and its composites is reported in Fig. 9. As expected, when the fibre content rises, the storage modulus increases and the loss factor decreases. As reported in Table 1, the temperature of the loss factor peak, that represents the glass transition temperature (T_g) of the rPET matrix, is slightly increasing with the fibre content. As for the tensile modulus, also the storage modulus results to be practically unaffected by hydrothermal aging at 70 °C at 80 and 100% RH and not reported. On the other hand, as reported in Fig. 10(a) and (b), the position and the intensity of the loss factor peaks, are affected by the selected hydrothermal aging conditions. In particular, Fig. 10(a) clearly shows how the T_g is increasing during hydrothermal aging both at 80 and 100% RH. This behaviour is most probably related to a chemi-crystallization process, as evidenced by DSC measurements reported in our previous paper on this subject [43]. In fact, the T_g of the amorphous phase in a semicrystalline polymers depends on the degree of crystallinity. In some cases, for example in virgin PET, when the degree of crystallinity increases from 2 to 65%, T_g rises from 80 to 125 °C [59]. In the present case the crystallinity content of the rPET matrix has been observed to increase from 30.4% to about 36.1% after 24 weeks of hydrothermal aging in water [43] and its T_g is correspondingly increasing from 92 °C up to 100 °C as evidenced by DMTA analysis. From Fig. 10(a) it can be also observed that within the first 2 weeks of hydrothermal exposure the T_g is slightly decreasing due to a prevailing plasticizing effects of diffusing water. This could also explain the increase of tensile strength (and tensile strain at break) observed for the rPET matrix in the initial time of exposure to water either at 80 and 100% RH. The molecular-motion restricting effects of crystallites is also responsible for the decrease of loss factor peak values observed for the rPET matrix and reported in Fig. 10(b). The immobilizing effect of short

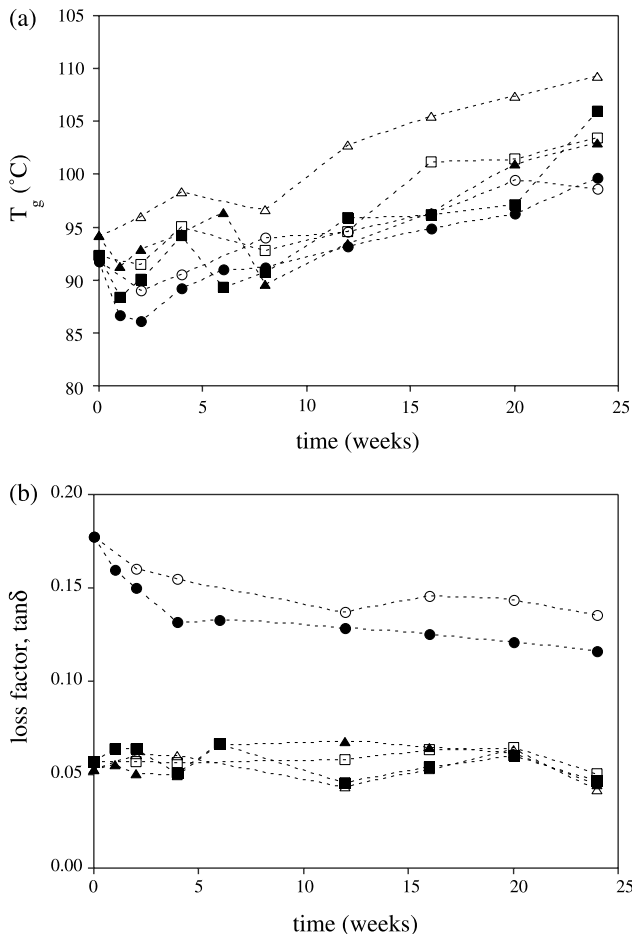


Fig. 10. Effect of hygrothermal aging time on (a) temperature of loss factor peak (T_g) and (b) loss factor peak values for: rPET at (○) 80% RH or (●) immersed in water; rPET-15GF at (□) 80% RH or (■) immersed in water; rPET-30GF at (△) 80% RH or (▲) immersed in water.

glass fibres may account for the lower loss factors values observed on rPET-15GF and rPET-30GF specimens, whose values are not substantially affected by the hygrothermal aging.

While the glass transition and melting temperatures define the behaviour of polymers and polymer composites from a scientific point of view, engineers frequently choose materials on the basis of more empirical parameters such as the heat deflection temperature (HDT) [60]. In fact, this is considered as a measure of the maximum service temperature of a polymeric material. One of the most striking effects due to fibres in composites is the great increase in heat distortion temperature [61]. In fact, as reported in Table 1, it is worth noting that the presence of glass fibres greatly increases the HDT values and that, for the higher fibre content of 30 wt%, values are comparable to those presented by commercial composites obtained with virgin PET [2]. HDT values show relatively small variations during aging time (see Fig. 11). In particular, for rPET matrix an increase of HDT values is observed up to values about 20% higher after 25 weeks of exposure for both humidity conditions

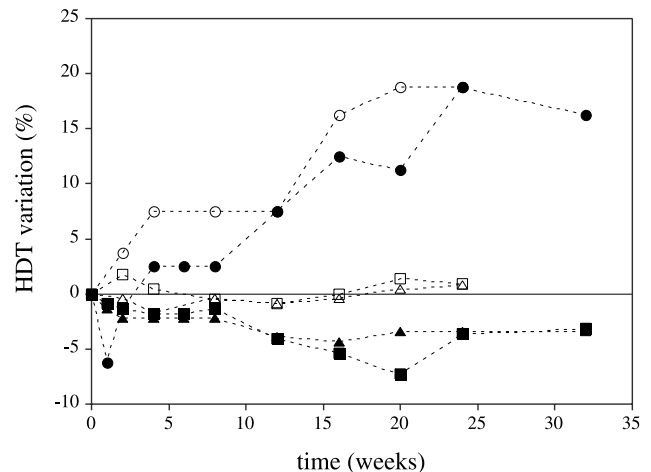


Fig. 11. Effect of aging time at 80 and 100% RH on HDT percent variation, for rPET and its composites for: rPET at (○) 80% RH or (●) immersed in water; rPET-15GF at (□) 80% RH or (■) immersed in water; rPET-30GF at (△) 80% RH or (▲) immersed in water.

This behaviour could be explained by assuming that the stiffening effect related to the chemicrystallization process is prevailing on the loss of mechanical properties related to the molar mass decrease. On the other hand, rPET composites immersed in water show a slight decrease of HDT values during aging time. This behaviour could be explained by considering that in glass fibre reinforced composites a further possible degradation mechanism has to be considered like the damage of the fibre/matrix interface in presence of diffusing water as confirmed by scanning electron microscopy observations (Fig. 8(b)).

4. Conclusions

From this investigation on the hygrothermal aging of rPET and its short glass fibres composites at 70 °C and 80 or 100% RH, the following conclusions can be drawn:

- (i) For all the investigated materials, the elastic mechanical properties (tensile and storage moduli) determined at low strain levels are practically constant over the entire period of hygrothermal exposure.
- (ii) A marked reduction of the tensile strength and apparent fracture toughness is observed for rPET matrix and its composites during hygrothermal aging at 80 and 100% RH; both properties depend on the molar mass of the rPET matrix, that decreases for the hydrolysis process during hygrothermal aging.
- (iii) The materials glass transition evaluated as the temperature of the loss factor peak is increasing during hygrothermal aging for the occurrence of a chemicrystallization process that causes an increase of the crystallinity content and a consequent reduction of the mobility of the amorphous phase.
- (iv) Consistently with the mechanical measurements,

morphology of fracture surfaces exposed to hygrothermal aging in water reveals a reduction of plastic deformation of the rPET matrix and a weakening of the fibre–matrix interface for rPET composites.

Acknowledgements

This work was carried out with the financial support of the ‘Ministero dell’Istruzione dell’Università e della Ricerca’ (MIUR-Italy), COFIN 2000 (Grant No. MM09012922_005). The authors sincerely wish to thank Mr. Stefano Bonafini for conducting most of the experimental work and Dr. Gianluca Gottardi of Eco Selekt Europa Srl (Salerno-Italy) for the help in materials preparation.

References

- [1] Gupta VB, Bashir Z. In: Fakirov S, editor. PET fibers, films, and bottles. Handbook of thermoplastic polyesters, vol. 1. Weinheim, Germany: Wiley-VCH; 2002. p. 317–88.
- [2] Rynite® PET Product Guide and Properties, DuPont Engineering Polymers. Available from <http://www.plastics.dupont.com/>, date of access August 2004.
- [3] Nadkarni VM. Recycling of polyesters. In: Fakirov S, editor. Handbook of thermoplastic polyesters, vol. 2. Weinheim, Germany: Wiley-VCH; 2002. p. 1223–49.
- [4] Paci M, La Mantia FP. Competition between degradation and chain extension during processing of reclaimed poly(ethylene terephthalate). Polym Degrad Stab 1998;61(3):417–20.
- [5] Available from: <http://www.corepla.it/ita/03/01.asp> date of access August 2004.
- [6] Spychaj T. Chemical recycling of PET: methods and products. In: Fakirov S, editor. Handbook of thermoplastic polyesters, vol. 2. Weinheim, Germany: Wiley-VCH; 2002. p. 1251–90.
- [7] Giannotta G, Po R, Cardi N, Tampellini E, Occhiello E, Garbassi F, Nicolais L. Processing effects on poly(ethylene-terephthalate) from bottle scraps. Polym Eng Sci 1994;34(15):1219–23.
- [8] Paci M, La Mantia FP. Influence of small amounts of polyvinylchloride on the recycling of polyethylene terephthalate. Polym Degrad Stab 1999;63(1):11–14.
- [9] Frounchi M. Studies on degradation of PET in mechanical recycling. Macromol Symp 1999;144:465–9.
- [10] Torres N, Robin JJ, Boutevin B. Study of thermal and mechanical properties of virgin and recycled poly(ethylene terephthalate) before and after injection molding. Eur Polym J 2000;36(10):2075–80.
- [11] Karger-Kocsis J. Recycling options for post-consumer PET and PET-containing wastes by melt blending. In: Fakirov S, editor. Handbook of thermoplastic polyesters, vol. 2. Weinheim, Germany: Wiley-VCH; 2002. p. 1291–318.
- [12] Abulsa IA, Jaynes CB, OGara JF. High-impact-strength poly(ethylene terephthalate) (PET) from virgin and recycled resins. J Appl Polym Sci 1996;59(13):1957–71.
- [13] Yu Z-Z, Yang M-S, Dai S-C, Mai Y-W. Toughening of recycled poly(ethylene terephthalate) with a maleic anhydride grafted SEBS triblock copolymer. J Appl Polym Sci 2004;93(3):1462–72.
- [14] Pegoretti A, Kolarik J, Gottardi G, Penati A. Heterogeneous blends poly(ethylene terephthalate)/impact modifier: phase structure and tensile creep. Polym Int 2004;53(7):984–94.
- [15] Laoutid F, Ferry L, Lopez-Cuesta JM, Crespy A. Red phosphorus/aluminium oxide compositions as flame retardants in recycled poly(ethylene terephthalate). Polym Degrad Stab 2003;82(2):357–63.
- [16] Pegoretti A, Kolarik J, Peroni C, Migliaresi C. Recycled poly(ethylene terephthalate)/layered silicate nanocomposites: morphology and tensile mechanical properties. Polymer 2004;45(8):2759–67.
- [17] Cantwell WJ. The fracture behaviour of glass fiber recycled PET composites. J Reinf Plast Compos 1999;18(4):373–87.
- [18] Jabarin SA, Logfren EA. Effects of water absorption on physical properties and degree of molecular orientation of poly(ethylene terephthalate). Polym Eng Sci 1986;26(9):620–5.
- [19] Edge M, Hayes M, Mohammadian M, Allen NS, Jewitt TS, Brems K, Jones K. Aspects of poly(ethylene terephthalate) degradation for archival life and environmental degradation. Polym Degrad Stab 1991;32(2):131–53.
- [20] Allen NS, Edge M, Mohammadian M, Jones K. Hydrolytic degradation of poly(ethylene terephthalate): importance of chain scission versus crystallinity. Eur Polym J 1991;27(12):1373–8.
- [21] Sawada S, Kamiyama K, Ohgushi S, Yabuki K. Degradation mechanisms of poly(ethylene terephthalate) tire yarn. J Appl Polym Sci 1991;42(4):1041–8.
- [22] Launay A, ThomINETTE F, Verdu J. Hydrolysis of poly(ethylene terephthalate)—a kinetic study. Polym Degrad Stab 1994;46(3):319–24.
- [23] Bellenger V, Ganem M, Mortaigne B, Verdu J. Lifetime prediction in the hydrolytic ageing of polyesters. Polym Degrad Stab 1995;49(1):91–7.
- [24] Launay A, ThomINETTE F, Verdu J. Hydrolysis of poly(ethylene terephthalate)—a steric exclusion chromatography study. Polym Degrad Stab 1999;46(3):319–24.
- [25] Barany T, Karger-Kocsis J, Czigany T. Effect of hygrothermal aging on the essential work of fracture response of amorphous poly(ethylene terephthalate). Polym Degrad Stab 2003;82(2):271–8.
- [26] Bastioli C, Guanella I, Romano G. Effects of water sorption on the physical properties of PET, PBT and their long fibres composites. Polym Compos 1990;11(1):1–9.
- [27] Bergeret A, Pires I, Foulc MP, Abadie B, Ferry L, Crespy A. The hygrothermal behaviour of glass–fibre-reinforced thermoplastic composites: a prediction of the composite lifetime. Polym Test 2001;20(7):753–63.
- [28] Mohd Ishak ZA, Lim NC. Effect of moisture absorption on the tensile properties of short glass-fiber-reinforced poly(butylene terephthalate). Polym Eng Sci 1994;34(22):1645–55.
- [29] Czigany T, Mohd Ishak ZA, Heitz T, Karger-Kocsis J. Effects of hygrothermal on the fracture and failure behaviour in short glass fibre reinforced, toughened poly(butylene terephthalate) composites. Polym Compos 1996;17(6):900–9.
- [30] Mohd Ishak ZA, Ishiaku US, Karger-Kocsis J. Hygrothermal aging and fracture behaviour of styrene–acrylonitrile/acrylate based core-shell rubber toughened poly(butylene terephthalate). J Appl Polym Sci 1999;74(10):2470–81.
- [31] Mohd Ishak ZA, Ishiaku US, Karger-Kocsis J. Hygrothermal aging and fracture behaviour of short-glass-fibre-reinforced rubber toughened poly(butylene terephthalate) composites. Compos Sci Technol 2000;60:803–15.
- [32] Mohd Ishak ZA, Tengku Mansor TSA, Yow BN, Ishiaku US, Karger-Kocsis J. Short glass fibre reinforced poly(butylene terephthalate). Part 1—microstructural characterisation and kinetics of moisture absorption. Plast Rubber Compos 2000;29(6):263–70.
- [33] Mohd Ishak ZA, Tengku Mansor TSA, Yow BN, Ishiaku US, Karger-Kocsis J. Short glass fibre reinforced poly(butylene terephthalate). Part 2—effect of hygrothermal aging on mechanical properties. Plast Rubber Compos 2000;29(6):271–7.
- [34] Mohd Ishak ZA, Ariffin A, Senawi R. Effects of hygrothermal aging and a silane coupling agent on the tensile properties of injection molded short glass fibre reinforced poly(butylene terephthalate) composites. Eur Polym J 2001;37(8):1635–47.

- [35] Yow BN, Ishiaku US, Mohd Ishak ZA, Karger-Kocsis J. Kinetics of water absorption and hygrothermal aging of rubber toughened poly(butylene terephthalate) with and without short glass fiber reinforcement. *J Appl Polym Sci* 2004;92(1):506–16.
- [36] Pecorini TJ, Hertzberg RW. The fracture toughness and fatigue-crack propagation behaviour of annealed PET. *Polymer* 1993;34(24):5053–62.
- [37] Moore WR, Sanderson D. Viscosities of dilute solutions of polyethylene terephthalate. *Polymer* 1968;9:153–8.
- [38] ASTM D 5045-99 Standard test methods for plane-strain fracture toughness and strain energy release rate of plastic materials.
- [39] Karger-Kocsis J. Microstructure and fracture mechanical performance of short-fiber reinforced thermoplastics. In: Friedrich K, editor. Application of fracture mechanics to composite materials. Amsterdam, The Netherlands: Elsevier; 1989. p. 189–247.
- [40] Evans WJ, Isaac DH, Saib KS. The effect of short carbon fibre reinforcement on crack growth in PEEK. *Compos Part A* 1996;27A:547–54.
- [41] Pegoretti A, Migliaresi C. Effect of hydrothermal aging on the thermo-mechanical properties of a composite dental prosthetic material. *Polym Compos* 2002;23(3):342–51.
- [42] Pegoretti A, Fambri L, Migliaresi C. In vitro degradation of poly(L-lactic acid) fibers produced by melt spinning. *J Appl Polym Sci* 1997;64:213–23.
- [43] Pegoretti A, Penati A. Effect of hygrothermal aging on the molar mass and thermal properties of recycled poly(ethylene terephthalate) and its short glass fibres composites. *Polym Degrad Stab* 2004 (in press).
- [44] Flory PJ. Tensile strength in relation to molecular weight of high polymers. *J Am Chem Soc* 1945;67:2048–50.
- [45] Vincent PI. The tough-brittle transition in thermoplastics. *Polymer* 1960;1:425–44.
- [46] Kausch HH. *Polymer fracture*. Berlin, Germany: Springer; 1987. p. 69.
- [47] Chu CC. Hydrolytic degradation of polyglycolic acid: tensile strength and crystallinity study. *J Appl Polym Sci* 1981;26:1727–34.
- [48] Pitt CG, Chasalow FJ, Hibionada YM, Klimas DM, Schindler A. Aliphatic polyesters. I. The degradation of poly(ϵ -caprolactone) in vivo. *J Appl Polym Sci* 1981;26:3779–87.
- [49] Mathisen T, Albertsson AC. Hydrolytic degradation of melt-extruded fibers from poly(β -propiolactone). *J Appl Polym Sci* 1990;39:591–601.
- [50] Grijpma DW, Nijenhuis AJ, Pennings AJ. Synthesis and hydrolytic degradation behaviour of high-molecular-weight L-lactide and glycolide copolymers. *Polymer* 1990;31:2201–6.
- [51] Lin HL, Chu CC, Grubb D. Hydrolytic degradation and morphologic study of poly-p-dioxanone. *J Biomed Mater Res* 1993;27:153–66.
- [52] Migliaresi C, Fambri L, Cohn D. A study on the in vitro degradation of poly(lactic acid). *J Biomed Sci Polym Ed* 1994;5(6):591–606.
- [53] Kinloch AJ, Young RJ. *Fracture behaviour of polymers*. London: Elsevier Science; 1983. p. 251–2.
- [54] Bucknall CB. *Toughened plastics*. London: Elsevier Science; 1977. p. 264–5.
- [55] deGennes PG. Toughness of glassy polymers: a tentative scheme. *Europhys Lett* 1991;15(2):191–6.
- [56] Tsui S-W, Duckett RA, Ward IM. Influence of molecular weight and branch content on the fracture behaviour of polyethylene. *J Mater Sci* 1992;27(10):2799–806.
- [57] Avella M, dell'Erba R, Martuscelli E, Ragosta G. Influence of molecular mass, thermal treatment and nucleating agent on structure and fracture toughness of isotactic polypropylene. *Polymer* 1993;34(14):2951–60.
- [58] Chivers RA, Moore DR. The effect of molecular weight and crystallinity on the mechanical properties of injection moulded poly(aryl-ether-ether-ketone) resin. *Polymer* 1994;35(1):110–6.
- [59] Riande E, Diaz-Calleja R, Prolongo MG, Masegosa RM, Salom C. *Polymer viscoelasticity*. New York: Marcel Dekker Inc; 1987. Chapter 2, p. 29–84.
- [60] Sperling LH. *Introduction to physical polymer science*, 3rd ed. New York: Wiley Interscience; 2001. Chapter 8, p. 295–362.
- [61] Nielsen LE, Landel RF. *Mechanical properties of polymers and composites*, 2nd ed. New York: Marcel Dekker; 1994. Chapter 8, p. 461–513.